The Astrophysical Journal Letters, 776:L33 (6pp), 2013 October 20 doi:10.1088/2041-8205/776/2/L33

MAGNETIC SHIELDING OF EXOMOONS BEYOND THE CIRCUMPLANETARY HABITABLE EDGE

René Heller[1] and Jorge I. Zuluaga[2]
[1] McMaster University, Department of Physics and Astronomy, Hamilton, ON L8S 4M1, Canada; rheller@physics.mcmaster.ca
[2] FACom - Instituto de Física - FCEN, Universidad de Antioquia, Calle 70 No. 52-21, Medellín, Colombia; jzuluaga@fisica.udea.edu.co
Received 2013 June 24; accepted 2013 August 11; published 2013 October 7

ABSTRACT

With most planets and planetary candidates detected in the stellar habitable zone (HZ) being super-Earths and gas giants rather than Earth-like planets, we naturally wonder if their moons could be habitable. The first detection of such an exomoon has now become feasible, and due to observational biases it will be at least twice as massive as Mars. However, formation models predict that moons can hardly be as massive as Earth. Hence, a giant planet's magnetosphere could be the only possibility for such a moon to be shielded from cosmic and stellar high-energy radiation. Yet, the planetary radiation belt could also have detrimental effects on exomoon habitability. Here we synthesize models for the evolution of the magnetic environment of giant planets with thresholds from the runaway greenhouse (RG) effect to assess the habitability of exomoons. For modest eccentricities, we find that satellites around Neptune-sized planets in the center of the HZ around K dwarf stars will either be in an RG state and not be habitable, or they will be in wide orbits where they will not be affected by the planetary magnetosphere. Saturn-like planets have stronger fields, and Jupiter-like planets could coat close-in habitable moons soon after formation. Moons at distances between about 5 and 20 planetary radii from a giant planet can be habitable from an illumination and tidal heating point of view, but still the planetary magnetosphere would critically influence their habitability.

Key words: astrobiology – celestial mechanics – methods: analytical – planets and satellites: magnetic fields – planets and satellites: physical evolution – planet–star interactions

Online-only material: color figures

1. INTRODUCTION

The search for life on worlds outside the solar system has experienced a substantial boost with the launch of the *Kepler* space telescope in 2009 March (Borucki et al. 2010). Since then, thousands of planet candidates have been detected (Batalha et al. 2013), several tens of which could be terrestrial and have orbits that would allow for liquid surface water (Kaltenegger & Sasselov 2011). The concept used to describe this potential for liquid water, which is tied to the search for life, is called the "habitable zone" (HZ; Kasting et al. 1993). Yet, most of the *Kepler* candidates, as well as most of the planets in the HZ detected by radial velocity measurements, are giant planets and not Earth-like. This leads us to the question whether these giants can host terrestrial exomoons, which may serve as habitats (Reynolds et al. 1987; Williams et al. 1997).

Recent searches for exomoons in the *Kepler* data (Kipping et al. 2013a, 2013b) have fueled the debate about the existence and habitability of exomoons and incentivized others to develop models for the surface conditions on these worlds. While these studies considered illumination effects from the star and the planet, as well as eclipses, tidal heating (Heller 2012; Heller & Barnes 2013a, 2013b), and the transport of energy in the moon's atmosphere (Forgan & Kipping 2013), the magnetic environment of exomoons has hitherto been unexplored.

Moons around giant planets are subject to high-energy radiation from (1) cosmic particles, (2) the stellar wind, and (3) particles trapped in the planet's magnetosphere (Baumstark-Khan & Facius 2002). Contributions (1) and (2) are much weaker inside the planet's magnetosphere than outside, but effect (3) can still have detrimental consequences. The net effect (beneficial or detrimental) on a moon's habitability depends on the actual orbit of the moon, the extent of the magnetosphere, the intrinsic magnetosphere of the moon, the stellar wind, etc.

Stellar mass-loss and X-ray and extreme UV (XUV) radiation can cause the atmosphere of a terrestrial world to be stripped off. Light bodies are in particular danger, as their surface gravity is weak and volatiles can escape easily (Lammer et al. 2013). Mars, for example, is supposed to have lost vast amounts of CO_2, N, O, and H (the latter two formerly bound as water; McElroy 1972; Pepin 1994; Valeille et al. 2010). Intrinsic and extrinsic magnetic fields can help moons sustain their atmospheres and they are mandatory to shield life on the surface against galactic cosmic rays (Grießmeier et al. 2009). High-energy radiation can also affect the atmospheric chemistry, thereby spoiling signatures of spectral biomarkers, especially of the ozone (Segura et al. 2010).

Understanding the evolution of the magnetic environments of exomoons is thus crucial to assess their habitability. Here we extend models recently applied to the evolution of magnetospheres around terrestrial planets under an evolving stellar wind (Zuluaga et al. 2013). Employed on giant planets, they allow us a first approach toward parameterizing the potential of a giant planet's magnetosphere to affect potentially habitable moons.

2. METHODS

In the following, we model a range of hypothetical systems to explore the potential of a giant planet's magnetosphere to embrace moons that are habitable from a tidal and energy budget point of view.

2.1. Bodily Characteristics of the Star

M dwarf stars are known to show strong magnetic bursts, eventually coupled with the emission of XUV radiation as well as other high-energy particles (Gurzadian 1970; Silvestri et al. 2005). Moreover, stars with masses below 0.2–0.5 solar masses ($M_\odot$) cannot possibly host habitable moons, since stellar perturbations excite hazardous tidal heating in the satellites

(Heller 2012). We thus concentrate on stars more similar to the Sun. G dwarfs, however, are likely too bright and too massive to allow for exomoon detections in the near future. As a compromise, we choose a 0.7 $M_\odot$ K dwarf star with solar metallicity $Z = 0.0152$ and derive its radius ($R_\star$) and effective temperature ($T_{\rm eff,\star}$) at an age of 100 Myr (Bressan et al. 2012): $R_\star = 0.597\ R_\odot$ ($R_\odot$ being the solar radius), $T_{\rm eff,\star} = 4270$ K. These values are nearly constant over the next couple of Gyr.

2.2. Bodily Characteristics of the Planet

We use planetary evolution models of Fortney et al. (2007) to explore two extreme scenarios, between which we expect most giant planets: (1) mostly gaseous with a core mass $M_{\rm c} = 10$ Earth masses ($M_\oplus$) and (2) planets with comparatively massive cores. Class (1) corresponds to larger planets for given planetary mass ($M_{\rm p}$). Models for suite (2) are constructed in the following way. For $M_{\rm p} < 0.3\ M_{\rm Jup}$, we interpolate between radii of planets with core masses $M_{\rm c} = 10$, 25, 50, and 100 $M_\oplus$ to construct Neptune-like worlds with a total amount of 10% hydrogen (H) and helium (He) by mass. For $M_{\rm p} > 0.3\ M_{\rm Jup}$, we take the precomputed $M_{\rm c} = 100\ M_\oplus$ grid of models. These massive-core planets (2) yield an estimate of the *minimum* radius for given $M_{\rm p}$. To account for irradiation effects on planetary evolution, we apply the Fortney et al. (2007) models for planets at 1 AU from the Sun.

As it is desirable to compare our scaling laws for the magnetic properties of giant exoplanets with known magnetic dipole moments of solar system worlds, we start out by considering a Neptune-, a Saturn-, and a Jupiter-class host planet. For the sake of consistency, we attribute total masses of 0.05, 0.3, and 1 $M_{\rm Jup}$, as well as $M_{\rm c} = 10$, 25, and again 10 $M_\oplus$, respectively.

2.3. Bodily Characteristics of the Moon

Kepler has been shown capable of detecting moons as small as 0.2 $M_\oplus$ combining measurements of the planet's transit timing variation and transit duration variation (Kipping et al. 2009). The detection of a planet as small as 0.3 Earth radii ($R_\oplus$), almost half the radius of Mars (Barclay et al. 2013), around a K star suggests that direct transit measurements of Mars-sized moons may be possible with current or near-future technology (Sartoretti & Schneider 1999; Szabó et al. 2006; Kipping 2011). Yet, in situ formation of satellites is restricted to a few times $10^{-4}\ M_{\rm p}$ at most (Canup & Ward 2006; Sasaki et al. 2010; Ogihara & Ida 2012). For a Jupiter-mass planet, this estimate yields a satellite of about 0.03 $M_\oplus \approx 0.3$ times the mass of Mars. Alternatively, moons can form via a range of other mechanisms (for a review, see Section 2.1 in Heller & Barnes 2013b). We therefore suspect moons of roughly the mass and size of Mars to exist and to be detectable in the near future.

Following Fortney et al. (2007) and assuming an Earth-like rock-to-mass fraction of 68%, we derive a radius of 0.94 Mars radii or 0.5 $R_\oplus$ for a Mars-mass exomoon. Tidal heating in the moon is calculated using the model of Leconte et al. (2010) and assuming an Earth-like time lag of the moon's tidal bulge $\tau_{\rm s} = 638$ s as well as a second degree tidal Love number $k_{2,\rm s} = 0.3$ (Heller et al. 2011).

2.4. The Stellar Habitable Zone

We investigate a range of planet–moon binaries located in the center of the stellar HZ. Therefore, we compute the arithmetic mean of the inner HZ edge (given by the moist greenhouse effect) and the outer HZ edge (given by the maximum greenhouse) around a K dwarf star (Section 2.1) using the model of Kopparapu et al. (2013). For this particular star, we localize the center of the HZ at 0.56 AU.

2.5. The Runaway Greenhouse and Io Limits

The tighter a moon's orbit around its planet, the more intense the illumination it receives from the planet and the stronger tidal heating. Ultimately, there exists a minimum circumplanetary orbital distance, at which the moon becomes uninhabitable, called the "habitable edge" (HE; Heller & Barnes 2013b). As tidal heating depends strongly on the orbital eccentricity $e_{\rm ps}$, amongst others, the radius of the "HE" also depends on $e_{\rm ps}$.

We consider two thresholds for a transition into an uninhabitable state. (1) When the moon's tidal heating reaches a surface flux similar to that observed on Jupiter's moon Io, that is 2 W m^{-2}, then enhanced tectonic activity as well as hazardous volcanism may occur. Such a scenario could still allow for a substantial area of the moon to be habitable, as tidal heat leaves the surface through hot spots, (see Io and Enceladus; Ojakangas & Stevenson 1986; Spencer et al. 2006; Tobie et al. 2008), and there may still exist habitable regions on the surface. Hence, we consider this "Io-limit HE" (Io HE) as a pessimistic approach. (2) When the moon's global energy flux exceeds the critical flux to become a runaway greenhouse (RG), then any liquid surface water reservoirs can be lost due to photodissociation into hydrogen and oxygen in the high atmosphere (Kasting 1988). Eventually, hydrogen escapes into space and the moon will be desiccated forever. We apply the semi-analytic RG model of Pierrehumbert (2010; see Equation (1) in Heller & Barnes 2013b) to constrain the innermost circumplanetary orbit at which a moon with given eccentricity would just be habitable. For our prototype moon, this model predicts a limit of 269 W m^{-2} above which the moon would transition to an RG state. We call the corresponding critical semimajor axis the "runaway greenhouse HE" (RG HE) and consider it as an optimistic approach.

We calculate the Io and RG HEs for $e_{\rm ps} \in \{0.1, 0.01, 0.001\}$ using Equation (22) from Heller & Barnes (2013b) and introducing two modifications. First, the planetary surface temperature ($T_{\rm p}$) depends on the equilibrium temperature ($T_{\rm p}^{\rm eq}$) due to absorbed stellar light and on an additional component ($T_{\rm int}$) from internal heating: $T_{\rm p} = ([T_{\rm p}^{\rm eq}]^4 + T_{\rm int}^4)^{1/4}$. Second, we use a Bond albedo $\alpha_{\rm opt} = 0.3$ for the stellar illumination absorbed by the moon and $\alpha_{\rm IR} = 0.05$ for the light absorbed from the relatively cool planet (Heller & Barnes 2013a).

2.6. Planetary Dynamos

We apply scaling laws for the magnetic field strength (Olson & Christensen 2006) that consider convection in a spherical conducting shell inside a giant planet and a convective power $Q_{\rm conv}$ (Equation (28) in Zuluaga et al. 2013), provided by the Fortney et al. (2007) models. The ratio between inertial forces to Coriolis forces is crucial in determining the field regime—whether it is dipolar- or multipolar-dominated—for the dipole field strength on the planetary surface. We scale the ratio between dipolar and total field strengths following Zuluaga & Cuartas (2012).

The core density ($\rho_{\rm c}$) is estimated by solving a polytropic model of index 1 (Hubbard 1984). Radius and extent of the convective region are estimated by applying a semi-empirical scaling relationship for the dynamo region (Grießmeier 2006).

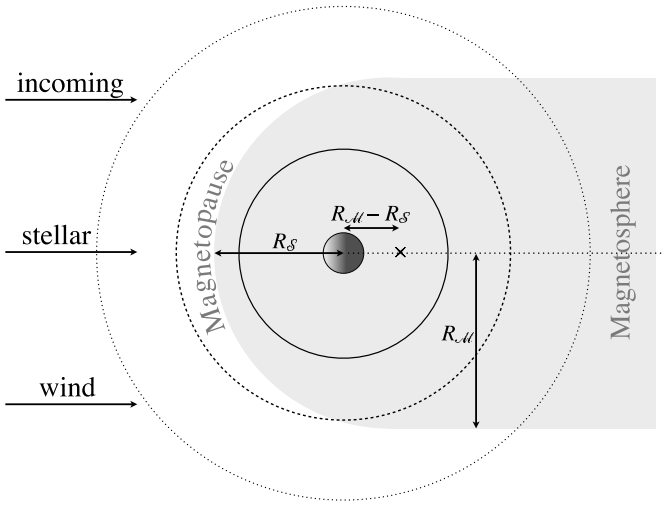

Figure 1. Illustration of the planetary magnetosphere. $R_{\mathcal{S}}$ denotes the standoff distance and $R_{\mathcal{M}}$ is the radius of the magnetopause. A range of satellite orbits illustrates how a moon can periodically dive into and out of the planetary magnetosphere. Conceptually, the dashed orbit resembles that of Titan around Saturn, with occasional shielding and exposition to the solar wind (Bertucci et al. 2008). At orbital distances $\gtrsim 2\,R_{\mathcal{S}}$, the fraction of the moon's orbit spent outside the planet's magnetospheric cavity reaches ≈80%.

Thermal diffusivity κ is assumed equal to 10^{-6} for all planets (Guillot 2005). Electrical conductivity σ is assumed to be 6×10^4 for planets rich in H and He, and $\sigma = 1.8\times10^4$ for the ice-rich giants (Olson & Christensen 2006).

We have verified that our model predicts dynamo regions that are similar to results obtained by more sophisticated analyses. For Neptune, our model predicts a dynamo radius $R_c = 0.77$ planetary radii (R_p) and $\rho_c = 3000\,\mathrm{kg\,m^{-3}}$, in good agreement to Kaspi et al. (2013). We also ascertained the dynamo scaling laws to reasonably reproduce the planetary dipole moments of Ganymede, Earth, Uranus, Neptune, Saturn, and Jupiter (J. I. Zuluaga et al., in preparation). For the mass range considered here, the predicted dipole moments agree within a factor of two to six. Discrepancies of this magnitude are sufficient for our estimation of magnetospheric properties, because they scale with $M_{\mathrm{dip}}^{1/3}$. Significant underestimations arise for Neptune and Uranus, which have strongly non-dipolar surface fields.

2.7. Evolution of the Magnetic Standoff Distance

The shape of the planet's magnetosphere can be approximated as a combination of a semi-sphere with radius $R_{\mathcal{M}}$ and a cylinder representing the tail region (Figure 1). The planet is at a distance $R_{\mathcal{M}} - R_{\mathcal{S}}$ off the sphere's center, with

$$R_{\mathcal{S}} = \left(\frac{\mu_0 f_0^2}{8\pi^2}\right)^{1/6} \mathcal{M}^{1/3} P_{\mathrm{sw}}^{-1/6} \qquad (1)$$

being the standoff distance, $\mu_0 = 4\pi\times10^{-7}\,\mathrm{N\,A^{-2}}$ the vacuum magnetic permeability, $f_0 = 1.3$ a geometric factor, $\mathcal{M}$ planetary magnetic dipole moment, and $P_{\mathrm{sw}} \propto n_{\mathrm{sw}} v_{\mathrm{sw}}$ the dynamical pressure of the stellar wind. Number densities n_{sw} and velocities v_{sw} of the stellar wind are calculated using a hydrodynamical model (Parker 1958). Both quantities evolve as the star ages. Thus, we use empirical formulae (Grießmeier et al. 2007) to parameterize their time dependence.

Observations of stellar winds from young stars are challenging, and thus the models only cover stars older than 700 Myr. We extrapolate these models back to 100 Myr, although there are indications that stellar winds "saturate" when going back in time (J. Linsky 2012, private communication).

3. RESULTS

3.1. Evolution of Magnetic Standoff Distance versus Runaway Greenhouse and Io Habitable Edges

Figure 2 visualizes the evolution of $R_{\mathcal{S}}$ (thick blue line) as a snail curling around the planet, indicated by a dark circle in the center. Stellar age ($t_\star$) is denoted in units of Gyr along the snail, starting at 0.1 Gyr at "noon" and ending after 4.6 Gyr at "midnight." $R_{\mathcal{S}}$, as well as the RG and Io HEs, are given in units of R_p. At $t_\star = 0.1$ Gyr ($t_\star = 4.6$ Gyr), $R_p = 0.385$, 1.023, and 1.195 R_{Jup} (0.329, 0.862, and 1.056 R_{Jup}) for the Neptune-, Saturn-, and Jupiter-like planets, respectively.

In panel (a) for the Neptune-like host, $R_{\mathcal{S}}$ starts very close to the planet and even inside the RG HE for the $e_{\mathrm{ps}} = 0.001$ case (thin black snail), at roughly $2\,R_p$ from the planetary center. This means that at an age of 0.1 Gyr, any Mars-like satellite with $e_{\mathrm{ps}} = 0.001$ would need to orbit beyond $2\,R_p$ to avoid transition into a RG state, where it would not be affected by the planet's magnetosphere. As the system ages, wider orbits are enshrouded by the planetary magnetic field, until after 4.6 Gyr, $R_{\mathcal{S}}$ reaches as far as the Io HE for $e_{\mathrm{ps}} = 0.1$ (thick dashed line).[3] In summary, moons in low-eccentricity orbits around Neptune-like planets can be close the planet and be habitable from an illumination and tidal heating point of view, but it will take at least 300 Myr in our specific case until they get coated by the planet's magnetosphere. Exomoons on more eccentric orbits will either be uninhabitable or affected by the planet's magnetosphere after more than 300 Myr.

Moving on to Figure 2(b) and the Saturn-like host, we find that $R_{\mathcal{S}}$ reaches the $e_{\mathrm{ps}} = 0.001$ RG HE after roughly 200 Myr, but it transitions all the other HEs substantially later than in the case of a Neptune-like host. After ≈1 Gyr, the $e_{\mathrm{ps}} = 0.01$ RG HE and the Io HE for $e_{\mathrm{ps}} = 0.01$ are transversed. After 4.6 Gyr, all orbits except for the Io HE at an eccentricity of 0.1 are covered by the planet's magnetic field. In conclusion, close-in Mars-sized moons around Saturn-like planets can be magnetically affected early on and be habitable from a RG or tidal heating point of view, if their orbital eccentricities are small.

Finally, Figure 2(c) shows that exomoons at the RG HE of Jovian planets for $e_{\mathrm{ps}} = 0.001$ will be bathed in the planetary magnetosphere at stellar ages as young as 100 Myr. After roughly 1.3 Gyr, $R_{\mathcal{S}}$ transitions the RG HE for $e_{\mathrm{ps}} = 0.1$ and the Io HE for $e_{\mathrm{ps}} = 0.01$. Even the Io HE with an eccentricity of $e_{\mathrm{ps}} = 0.1$ is covered at around 3.1 Gyr. After 4.6 Gyr, the planet's magnetic shield reaches as far as $21\,R_p$. Clearly, exomoons about Jupiter-like planets face the greatest prospects of interference with the planetary magnetosphere, even in orbits that are sufficiently wide to ensure negligible tidal heating.

3.2. Minimum Magnetic Dipole Moment

Looking at the standoff radii for the three cases in Figure 2, we wonder how strong the magnetic dipole moment $\mathcal{M}_{\mathrm{dip}}$ would need to be after 0.5 Gyr, when the atmospheric buildup should have mostly ceased, in order to magnetically enwrap the moon at a given HE. This question is answered in Figure 3.

[3] Note that as the planet shrinks, the RG and Io HEs also move outward. This is because of our visualization in units of planetary radii, while the values of the HEs remain constant in secular units.

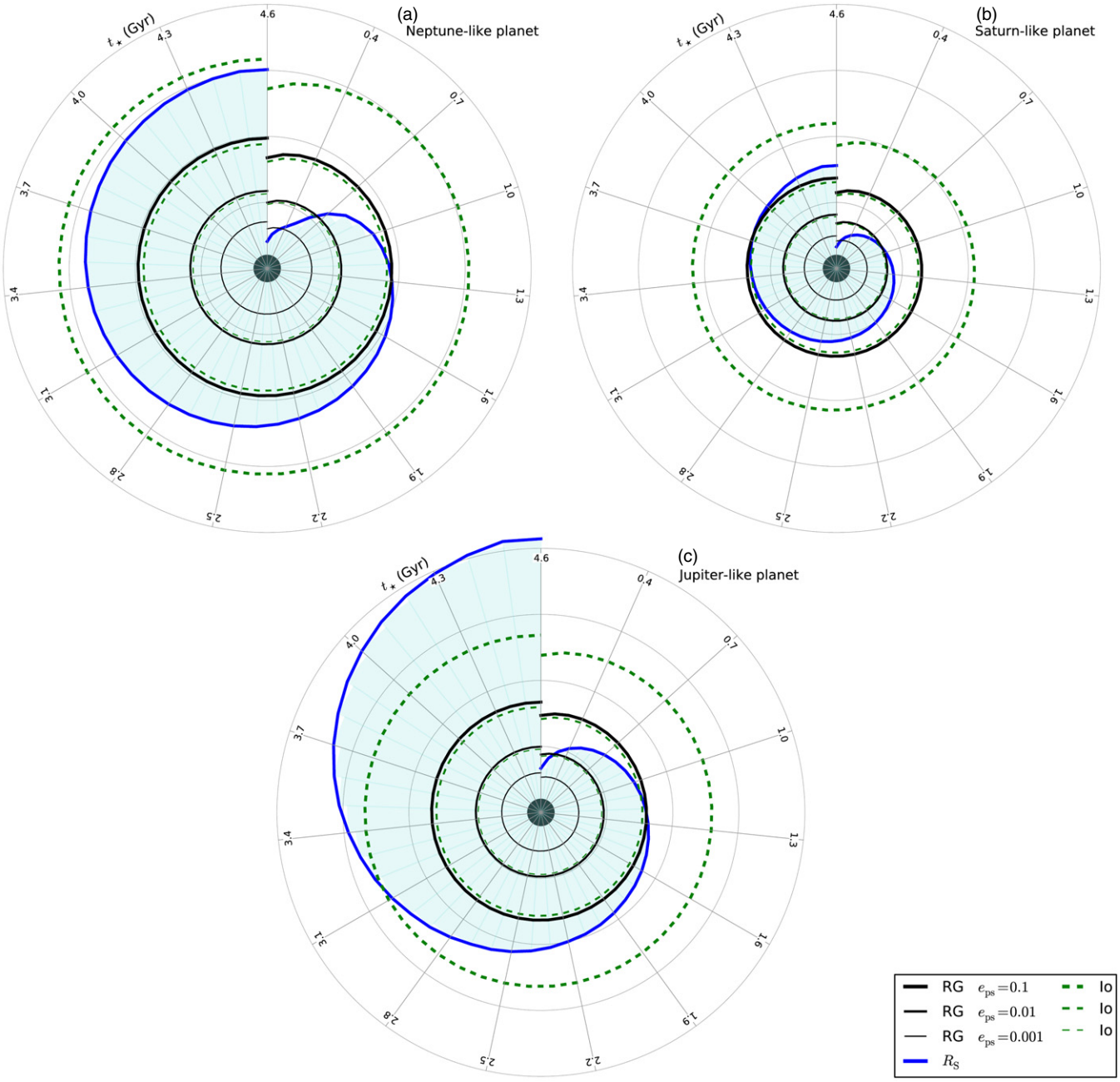

Figure 2. Evolution of the magnetic shielding (blue curves) compared to the RG HEs (solid black lines) and Io-like HEs (dashed green lines). Thick lines correspond to HEs for $e_{ps} = 0.1$, intermediate thickness to $e_{ps} = 0.01$, and thin circles to $e_{ps} = 0.001$. Thin gray lines denote distances in intervals of 5 planetary radii. The filled circle in the center symbolizes the planetary radius. Panel (a) shows a Neptune-like host, (b) a Saturn-like planet, and (c) a Jupiter-like planet. In all computations, a Mars-sized moon is assumed, and the planet–moon binary orbits a K dwarf in the center of the stellar HZ.

(A color version of this figure is available in the online journal.)

While planets with relatively massive cores (brown solid line) shield a wider range of orbits for given M_p below roughly 1 M_{Jup}, the low-mass core model (blue solid line) catches up for more massive giants. What is more, our model tracks for the predicted M_{dip}, which we expect to be located between the thick brown and thick blue line, "overtake" the RG and Io-like HEs for a range of eccentricities. HE contours that fall within the shaded area are magnetically protected, while moons above a certain HE are habitable from a tidal and illumination point of view.

We finally examine temporal aspects of magnetic shielding in Figure 4. The question answered in this plot is "how long would it take a planet to magnetically coat its moon beyond the HEs?" Again, planetary mass is along the abscissa, but now stellar lifetime $t_\star$ is along the ordinate. Clearly, the magnetic standoff radius of lower-mass planets requires more time to expand out to the respective HEs. While low-mass giants with low-mass cores (blue lines) require up to 3.5 Gyr to reach the RG HE for $e_{ps} = 0.01$, equally mass planets but with a high-mass core (thin brown line) could require as few as 650 Myr.

Planets more massive than roughly 0.3 M_{Jup} will coat their moons at the RG HE for $e_{ps} = 0.01$ as early as 1 Gyr after formation. For lower eccentricities, timescales decrease. As the RG HE is more inward to the planet than the Io HE, it is coated earlier than the Io limit for given e_{ps}. RG and Io

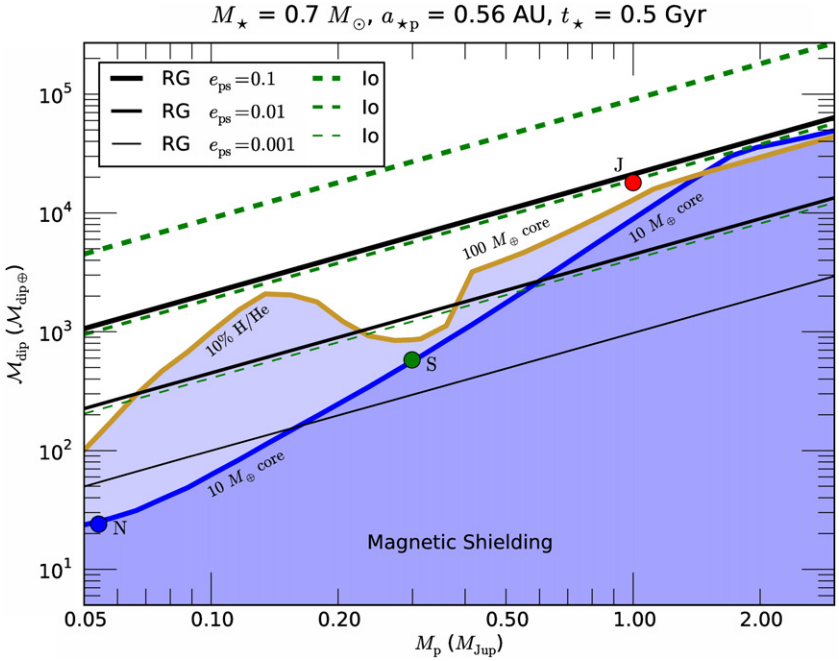

Figure 3. Magnetic dipole moments (ordinate) for a range of planetary masses (abscissa). The straight lines depict $\mathcal{M}_{dip}$ as it would be required at an age of 0.5 Gyr in order to shield a moon at a given HE (solid: runaway greenhouse; dashed: Io-like heating). Low-mass giants obviously fail to protect their moons beyond most HEs, while Jupiter-like planets offer a range of shielded orbits beyond the RG and Io HEs. Neptune, Saturn, and Jupiter are indicated with filled circles.

(A color version of this figure is available in the online journal.)

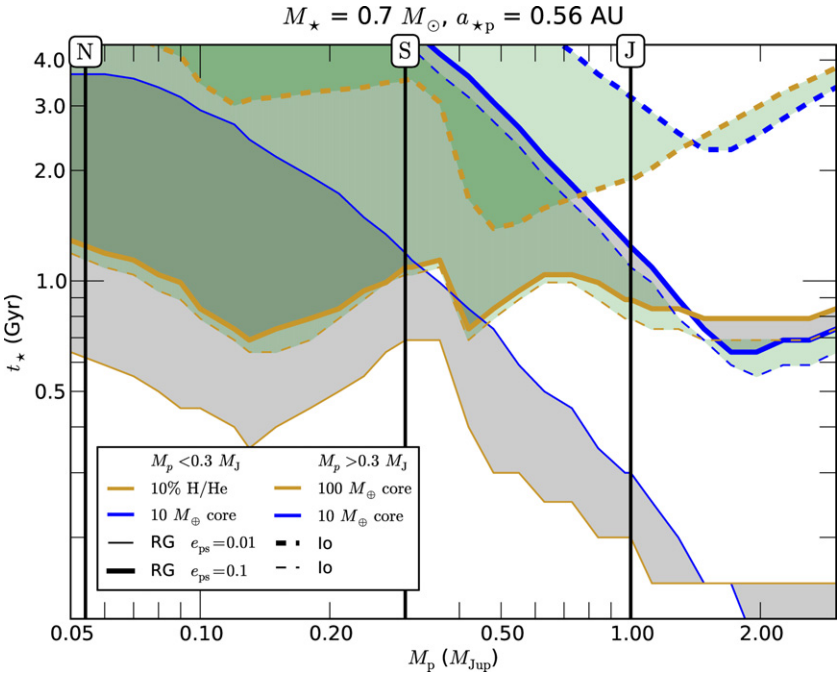

Figure 4. Time required by the planet's magnetic standoff radius R_S to envelop the Io (dashed) and RG (solid) HEs. Shaded regions illustrate uncertainties coming from planetary structure models, with the boundaries corresponding to a high- and a low-core mass planetary model, respectively (brown and blue lines). In general, the magnetic standoff distance around more massive planets requires less time to enshroud moons at a given HE.

(A color version of this figure is available in the online journal.)

HEs for $e_{ps} = 0.001$ are not shown as they are covered earlier than ≈300 Myr in all cases.

4. CONCLUSION

Mars-sized exomoons of Neptune-sized exoplanets in the stellar HZ of K stars will hardly be affected by planetary magnetospheres if these moons are habitable from an illumination and tidal heating point of view. While the magnetic standoff distance expands for higher-mass planets, ultimately Jovian hosts can enshroud their massive moons beyond the HE, depending on orbital eccentricity. In any case, exomoons beyond about 20 R_p will be habitable in terms of illumination and tidal heating, and they will not be coated by the planetary magnetosphere within

about 4.5 Gyr. Moons between 5 and 20 R_p can be habitable, depending on orbital eccentricity, and be affected by the planetary magnetosphere at the same time.

Uncertainties in the parameterization of tidal heating cause uncertainties in the extent of both the RG and Io HEs. Once a potentially habitable exomoon would be discovered, detailed interior models for the satellite's behavior under tidal stresses would need to be explored.

In a forthcoming study, we will examine the evolution of planetary dipole fields, and we will apply our methods to planets and candidates from the *Kepler* sample. Obviously, a range of giant planets resides in their stellar HZs, and these planets need to be prioritized for follow-up search on the potential of their moons to be habitable.

The referee report of Jonathan Fortney substantially improved the quality of this study. We have made use of NASA's ADS Bibliographic Services. Computations have been performed with `ipython 0.13` on `python 2.7.2` (Pérez & Granger 2007). R. H. receives funding from the Canadian Astrobiology Training Program. J.I.Z. is supported by CODI-UdeA and Colciencias.

REFERENCES

Barclay, T., Rowe, J. F., Lissauer, J. J., et al. 2013, Natur, 494, 452
Batalha, N. M., Rowe, J. F., Bryson, S. T., et al. 2013, ApJS, 204, 24
Baumstark-Khan, C., & Facius, R. 2002, in Life under Conditions of Ionizing Radiation, ed. G. Horneck & C. Baumstark-Khan (Berlin: Springer), 261
Bertucci, C., Achilleos, N., Dougherty, M. K., et al. 2008, Sci, 321, 1475
Borucki, W. J., Koch, D., Basri, G., et al. 2010, Sci, 327, 977
Bressan, A., Marigo, P., Girardi, L., et al. 2012, MNRAS, 427, 127
Canup, R. M., & Ward, W. R. 2006, Natur, 441, 834
Forgan, D., & Kipping, D. 2013, MNRAS, 432, 2994
Fortney, J. J., Marley, M. S., & Barnes, J. W. 2007, ApJ, 659, 1661
Grießmeier, J.-M. 2006, PhD thesis, Technische Universität Braunschweig
Grießmeier, J.-M., Preusse, S., Khodachenko, M., et al. 2007, P&SS, 55, 618
Grießmeier, J.-M., Stadelmann, A., Grenfell, J. L., Lammer, H., & Motschmann, U. 2009, Icar, 199, 526
Guillot, T. 2005, AREPS, 33, 493
Gurzadian, G. A. 1970, BOTT, 5, 263
Heller, R. 2012, A&A, 545, L8
Heller, R., & Barnes, R. 2013a, IJAsB, submitted
Heller, R., & Barnes, R. 2013b, AsBio, 13, 18
Heller, R., Leconte, J., & Barnes, R. 2011, A&A, 528, A27
Hubbard, W. B. 1984, Planetary Interiors (New York: Van Nostrand-Reinhold)
Kaltenegger, L., & Sasselov, D. 2011, ApJL, 736, L25
Kaspi, Y., Showman, A. P., Hubbard, W. B., Aharonson, O., & Helled, R. 2013, Natur, 497, 344
Kasting, J. F. 1988, Icar, 74, 472
Kasting, J. F., Whitmire, D. P., & Reynolds, R. T. 1993, Icar, 101, 108
Kipping, D. M. 2011, MNRAS, 416, 689
Kipping, D. M., Forgan, D., Hartman, J., et al. 2013a, arXiv:1306.1530
Kipping, D. M., Fossey, S. J., & Campanella, G. 2009, MNRAS, 400, 398
Kipping, D. M., Hartman, J., Buchhave, L. A., et al. 2013b, ApJ, 770, 101
Kopparapu, R. K., Ramirez, R., Kasting, J. F., et al. 2013, ApJ, 765, 131
Lammer, H., Kislyakova, K. G., Güdel, M., et al. 2013, in The Early Evolution of the Atmospheres of Terrestrial Planets, ed. J. M. Trigo-Rodriguez, F. Raulin, C. Muller, & C. Nixon (New York: Springer), 33
Leconte, J., Chabrier, G., Baraffe, I., & Levrard, B. 2010, A&A, 516, A64
McElroy, M. B. 1972, Sci, 175, 443
Ogihara, M., & Ida, S. 2012, ApJ, 753, 60
Ojakangas, G. W., & Stevenson, D. J. 1986, Icar, 66, 341
Olson, P., & Christensen, U. R. 2006, E&PSL, 250, 561
Parker, E. N. 1958, ApJ, 128, 664
Pepin, R. O. 1994, Icar, 111, 289
Pérez, F., & Granger, B. E. 2007, Comput. Sci. Eng., 9, 21
Pierrehumbert, R. T. 2010, Principles of Planetary Climate (New York: Cambridge Univ. Press)
Reynolds, R. T., McKay, C. P., & Kasting, J. F. 1987, AdSpR, 7, 125
Sartoretti, P., & Schneider, J. 1999, A&AS, 134, 553
Sasaki, T., Stewart, G. R., & Ida, S. 2010, ApJ, 714, 1052
Segura, A., Walkowicz, L. M., Meadows, V., Kasting, J., & Hawley, S. 2010, AsBio, 10, 751
Silvestri, N. M., Hawley, S. L., & Oswalt, T. D. 2005, AJ, 129, 2428
Spencer, J. R., Pearl, J. C., Segura, M., et al. 2006, Sci, 311, 1401
Szabó, G. M., Szatmáry, K., Divéki, Z., & Simon, A. 2006, A&A, 450, 395
Tobie, G., Čadek, O., & Sotin, C. 2008, Icar, 196, 642
Valeille, A., Bougher, S. W., Tenishev, V., Combi, M. R., & Nagy, A. F. 2010, Icar, 206, 28
Williams, D. M., Kasting, J. F., & Wade, R. A. 1997, Natur, 385, 234
Zuluaga, J. I., Bustamante, S., Cuartas, P. A., & Hoyos, J. H. 2013, ApJ, 770, 23
Zuluaga, J. I., & Cuartas, P. A. 2012, Icar, 217, 88